Tumor Pigmentation Does Not Affect Light-Activated Belzupacap Sarotalocan Treatment but Influences Macrophage Polarization in a Murine Melanoma Model

Sen Ma,[1] Ruben V. Huis in't Veld,[1–3] Yang Hao,[2,4] Zili Gu,[2] Cadmus Rich,[5] Maria Chiara Gelmi,[1] Aat A. Mulder,[6] Peter A. van Veelen,[7] T. Khanh H. Vu,[1] Thorbald van Hall,[8] Ferry A. Ossendorp,[3] and Martine J. Jager[1]

[1]Department of Ophthalmology, Leiden University Medical Center (LUMC), Leiden, The Netherlands
[2]Department of Radiology, Leiden University Medical Center (LUMC), Leiden, The Netherlands
[3]Department of Immunology, Leiden University Medical Center (LUMC), Leiden, The Netherlands
[4]Department of Laboratory Animals, College of Animal Sciences, Jilin University, Changchun, China
[5]Aura Biosciences, Inc., Boston, Massachusetts, United States
[6]Department of Electron Microscopy, Leiden University Medical Center (LUMC), Leiden, The Netherlands
[7]Center for Proteomics and Metabolomics, Leiden University Medical Center (LUMC), Leiden, The Netherlands
[8]Department of Medical Oncology, Oncology Institute, Leiden University Medical Center (LUMC), Leiden, The Netherlands

Correspondence: Martine J. Jager, Department of Ophthalmology, Leiden University Medical Center (LUMC), Albinusdreef 2, Leiden 2333 ZA, The Netherlands; m.j.jager@lumc.nl.

Received: September 15, 2023
Accepted: December 21, 2023
Published: January 25, 2024

Citation: Ma S, Huis in't Veld RV, Hao Y, et al. Tumor pigmentation does not affect light-activated Belzupacap sarotalocan treatment but influences macrophage polarization in a murine melanoma model. *Invest Ophthalmol Vis Sci.* 2024;65(1):42. https://doi.org/10.1167/iovs.65.1.42

Purpose. Pigmentation in uveal melanoma is associated with increased malignancy and is known as a barrier for photodynamic therapy. We investigated the role of pigmentation in tumor behavior and the response to light-activated Belzupacap sarotalocan (Bel-sar) treatment in a pigmented (wild type) and nonpigmented (tyrosinase knock-out [TYR knock-out]) cell line in vitro and in a murine model.

Methods. The B16F10 (TYR knock-out) was developed using CRISPR/Cas9. After the treatment with light-activated Bel-sar, cytotoxicity and exposure of damage-associated molecular patterns (DAMPs) were measured by flow cytometry. Treated tumor cells were co-cultured with bone marrow-derived macrophages (BMDMs) and dendritic cells (DCs) to assess phagocytosis and activation. Both cell lines were injected subcutaneously in syngeneic C57BL/6 mice.

Results. Knock-out of the tyrosinase gene in B16F10 led to loss of pigmentation and immature melanosomes. Pigmented tumors contained more M1 and fewer M2 macrophages compared with amelanotic tumors. Bel-sar treatment induced near complete cell death, accompanied with enhanced exposure of DAMPs in both cell lines, resulting in enhanced phagocytosis of BMDMs and maturation of DCs. Bel-sar treatment induced a shift to M1 macrophages and delayed tumor growth in both in vivo tumor models. Following treatment, especially the pigmented tumors and their draining lymph nodes contained IFN-gamma positive CD8+T cells.

Conclusions. Pigmentation influenced the type of infiltrating macrophages in the tumor, with more M1 macrophages in pigmented tumors. Belzupacap sarotalocan treatment induced immunogenic cell death and tumor growth delay in pigmented as well as in nonpigmented models and stimulated M1 macrophage influx in both models.

Keywords: eye, oncology, pigmentation, melanoma, light-activated, Belzupacap sarotalocan (Bel-sar)

Uveal melanoma (UM) is the most common primary ocular malignancy in adults and is often lethal.[1,2] Pigmentation is a bad prognostic factor and associated with high-risk genetic characteristics, such as loss of one chromosome 3 and loss of BAP1 expression in UM.[3] It is as yet unclear whether pigmentation is only a bystander effect of mutations in UM or plays a role in its dissemination. Pigmentation is not only a bad prognostic factor in UM but is known as a barrier for applying photodynamic therapy.[4] Clinical trials may therefore specifically target amelanotic melanoma.[5] Melanin is an effective quencher of singlet oxygen, which can protect melanocytes or melanoma cells from reactive oxygen species (ROS) induced, for example, by ultraviolet light and photodynamic therapy (PDT).[6,7] Pigmentation absorbs light across broad wavelengths and limits light penetration into tissues. Still, some photosensitizers, such as verteporfin (VP) and chlorines are effective against some pigmented cutaneous and UM.[8,9] In PDT, a photosensitizer is activated by a specific wavelength of exciting light in the presence of oxygen to produce ROS,

capable of causing intracellular oxidative stress and directly triggering tumor cell death or vascular damage.[10,11] In addition, the exposure and release of damage-associated molecular patterns (DAMPs) induced by PDT can trigger a strong local inflammatory response.[12,13] DAMPs, such as calreticulin (CRT), are known to act as an "eat me" signal to macrophages, enhancing phagocytosis of tumor cells.[14] CRT and other DAMPs, such as heat shock proteins (HSPs), may induce maturation of dendritic cells (DCs) which can activate a systemic immune response.[15] A stronger local inflammatory response triggered by PDT may contribute to immune activation. We recently published a paper stating that combining either PDT or light-activated Belzupacap sarotalocan (Bel-sar) with an immune checkpoint inhibitor induces a better antitumor response in mice than either treatment alone.[16,17]

Macrophages constitute an important type of infiltrating immune cell in malignancies and are considered to be highly plastic cells, which can be activated in response to different signals.[18] In UMs, high numbers of mainly M2 macrophages accompany heavy pigmentation and are associated with the development of metastases.[19–22] Macrophages have various functions: M1-type macrophages are able to destroy tumor structures by phagocytosis, elicit vascular damage, and tumor necrosis, whereas M2-type macrophages have the potential to enhance angiogenesis and induce immune suppression.[18,23] A stronger local inflammation triggered by PDT could contribute to the polarization of M2 macrophages to M1 macrophages, which could overcome a local immunosuppressive environment. This is important as the eye and intraocular UM are considered as immunosuppressive areas.[24,25]

The virus-like drug conjugate (VDC) Bel-sar (previously known as AU-011) is being used for the treatment of UM and indeterminate choroidal pigmented lesions[26–28] (ClinicalTrials.gov: NCT02422979). The VDC includes a human papilloma-virus derived empty capsid shell conjugated with approximately 200 molecules of a phthalocyanine photosensitizer. The virus-derived L1 and L2 proteins that comprise the virus capsid shell component of Bel-sar can specifically target malignant cells by binding to specifically modified glycosaminoglycans on heparan-sulfate proteoglycans (HSPG), which are preferentially expressed on tumor cells and are typically not present in normal healthy tissues. Following irradiation with a wavelength of 690 nm laser, the conjugated phthalocyanine photosensitizer is activated, resulting in the generation of ROS and, subsequently, acute cellular necrosis. This acute necrosis results in the release of tumor neoantigens and DAMPs and generates a long-lasting antitumor immunity.[27] The selectivity of Bel-sar reduces the risk of off-target effects and its application in the suprachoroidal space minimizes damage to the normal ocular structures, which are vital to preserve a patient's vision.

We wondered how pigmentation might affect Bel-sar treatment, and therefore set out to define the difference in in vitro and in vivo growth characteristics between two cell lines with and without pigment. UM and cutaneous melanoma (CM) arise from melanocytes that share the same embryonic origin and display the same cellular functions. However, UM and CM carry different mutations: UM typically have mutations in GNA11/GNAQ and a low mutational burden, whereas CM frequently have BRAF and NRAS mutations and a high mutational burden. The low mutation burden and hyperpigmentation of the murine-derived cutaneous B16F10 cell line makes it the ideal model for the preclinical study of UM, even if it lacks the specific mutations.[2]

We subsequently tested the effect of light-induced damage with Bel-sar treatment on cell line-derived tumors in a murine model, analyzing their growth and immune cell constitution.

Materials and Methods

Generation of Tyrosinase-Gene Knock-Out Cells

CRISPR/Cas9 sgRNA's targeting TYR were designed using the clustered regularly interspaced short palindromic repeats (CRISPR) design software (http://crispr.mit.edu). The sgRNA sequence (5′ CGGTCATCCACCCCTTTGA-3′) was cloned into a sgRNA expression vector (Addgene 41824) using a Gibson In-Fusion kit. B16F10 cells were transfected with the vector containing the sgRNA and a plasmid containing Cas9 (Addgene 41815) using lipofectamine 2000; the edited cells were selected using puromycin, then, a 96-well plate was used to dilute the B16F10 TYR gene knock-out cells. The mRNA analysis of cells transfected with the sgRNA/CAS9 plasmids showed the generation of TYR-deficient clonal cell populations. Sanger DNA sequencing was used to compare the B16F10 TYR gene knock-out and wild type cells and a single-cell colony with TYR knock-out was successfully acquired. The B16F10 wild type and B16F10 TYR knock-out cell lines were used for further experiments.

Cell Lines and Cell Culture

Tumor B16F10 cells and B16F10 knock-out cells after TYR knock-out (see above) were cultured under 5% CO_2 at 37°C in Dulbecco's Modified Eagle Medium (DMEM; Life Technologies) supplemented with 10% heat-inactivated fetal calf serum (Greiner Bio-One) and 1% penicillin/streptomycin (Life Technologies). The B16F10 cell line (ATCC CCL-6475) was acquired from the ATCC (Manassas, VA, USA).

Growth Curves In Vitro

Cells were seeded in a 6-well plate at a density of 25,000 cells/mL in 2 mL. On days 1, 2, 3, and 4, cell numbers were determined using the cell counter (NucieoCounter NC-300; Chemometec). Experiments were performed in triplicate.

Pigment Visualization in Cell Pellets or by Light Microscopy and Ultrastructural Analysis of Melanosomes by Electron Microscopy

To evaluate the pigmentation level in wild type and TYR knock-out melanoma cells, cells were pelleted by centrifugation (centrifuge at 500 G) and visually compared for cell and medium color. Light microscopy was used to visualize the intracellular or extracellular pigmentation of cultured cells.

In order to determine the effect of tyrosinase knock-out on the maturation of melanosomes, we applied transmission electron microscopy to observe their morphology.[29] Cells were fixed with 1.5% glutaraldehyde in 0.1 M cacodylate buffer for an hour at room temperature. After rinsing with 0.1 M cacodylate buffer 3 times, the cells were postfixed with 1% osmium tetroxide/1.5 potassium hexacyanoferrate (III) in 0.1 M cacodylate buffer. Cells were scraped from the T75 flasks and centrifuged into a pellet with 2% agar in MilliQ.

Investigative Ophthalmology & Visual Science

The pellet was cut into small parts of about 1 mm^3 and dehydrated with a series of ethanol and after that with a series of acetone/EPON (LX112, Leadd) and finally pure EPON. The pellets were placed in BEEM capsules with EPON and polymerized at 70°C for 48 hours. Then, 90 nm sections were processed and after staining with uranyl acetate and lead citrate, they were examined in a Tecnai 12 transmission electron microscope (Thermo Fisher). Overlapping images were automatically collected and stitched together into composite images, as previously described.[30]

Melanocyte Differentiation Antigen Expression Determined by Proteomic Analysis

Cells were cultured in a T75 flask and when the confluence reached 75%, the proteins were isolated and analyzed by mass spectrometry, as described.[31] Then, the raw data were analyzed by proteome discoverer version 2.2 (Thermo Electron). The presence of tyrosinase and other melanocyte differentiation antigens (microphthalmia-associated transcription factor [MITF], tyrosinase-related protein 1 [TYRP-1], tyrosinase-related protein 2 [TYRP-2], glycoprotein 100 [gp-100], and Melan-A) was determined by proteomics analysis.[32]

Binding and Uptake of Bel-Sar

Cells were seeded in 96-well plates (Greiner Bio-One) at 5000 cells per well and allowed to attach for 24 hours. They were then incubated with different concentrations (ranging from 3 pM to 900 pM) of Bel-sar during the indicated time periods at 4°C (binding) or 37°C (uptake). After the indicated time period, the cells were washed with phosphate-buffered saline (PBS) and fixed with 4% formalin (J.T. Baker) for 30 minutes. The cells were washed 3 times and reconstituted in 100 µl FACS buffer (PBS with 0.5% bovine serum albumin [BSA] and 0.02% sodium azide). The fluorescence of Bel-sar was then measured by LSR-II (BD Biosciences) in the APC-Cy7 channel.

In Vitro Cytotoxicity and Measurement of DAMP Exposure

To detect the cytotoxicity and immunogenic cell death induced by Bel-sar treatment, 5×10^4 B16F10 wild type or B16F10 TYR knock-out cells were seeded in a 24-well plate (Corning) and allowed to attach overnight in an incubator. The next day, the tumor cells were incubated with specific concentrations of Bel-sar for 4 hours, washed 3 times in PBS, and supplied with DMEM medium. Immediately after, they were irradiated with a 690 nm laser at a fluence rate of 400 mW/cm^2 for a total light fluence of $25J/cm^2$.

After 24 hours, cells were stained with propidium iodide (PI) and Annexin V-FITC (BD Pharmingen) in an Annexin V-binding buffer (Thermo Fisher). For immunogenic cell death, the cells were stained with Recombinant PE Anti-Calreticulin antibody (Abcam), or Recombinant Alexa 488-HSP90 antibody (Abcam). The samples were analyzed by flow cytometry on an LSR-II (BD Biosciences).

Phagocytosis and Maturation Assay

To detect potential differences in phagocytosis of Bel-sar treated pigmented and nonpigmented melanoma cells, we used a system with cultured immature dendritic cells (D1DCs) and bone marrow-derived macrophages (BMDMs). Briefly, tumor cells were first stained with CMFDA (1 uM, Chloromethylfluorescein diacetate; Abcam) for 1 hour and then treated with Bel-sar and laser as described above. Immediately thereafter, tumor cells were collected and co-cultured with D1DCs or BMDMs at a ratio of 1:1 or 1:5 for 2 hours. Cells were collected and stained with anti-CD11c-APC-ef780 (DC marker, clone N418; Thermo Fisher) or anti-CD11b-APC-ef780 (macrophage marker, clone M1/70; BD Biosciences) or anti-F4/80-PE-cy7 (macrophage marker, clone BM8; Thermo Fisher), and then analyzed by flow cytometry on an Aurora cytometer (Cytek Biosciences). The DCs or BMDMs that had phagocytosed tumor cells were CD11c+CMFDA+ or CD11b+F4/80+CMFDA+ positive, respectively. BMDMs were isolated from naïve adult C57BL/6 mice according to a standard protocol.[33]

To evaluate D1DC maturation, Bel-sar treated or Freeze-thawed melanoma cells were added to D1DCs at the ratio of 1:5 and co-cultured for 24 hours. Then, the cells were collected, stained with anti-CD11c-APC-ef780, anti-CD86-PE-cy7 (clone GL1, BD Biosciences), or anti-I-Ab-PE (major histocompatibility complex [MHC] class II; Clone M5/114.15.2; Thermo Fisher), and analyzed by flow cytometry on an Aurora cytometer (Aurora, Cytek Biosciences).

In Vivo Tumor Models

C57BL/6 mice were purchased from Janvier, The Netherlands, housed in pathogen-free animal facilities at the Leiden University Medical Center (LUMC), and used at 6 to 12 weeks of age. The animal experiments were approved by the animal Experimentation Committee of the LUMC (AVD 1160020198405). The animal experiments were carried out based on the guidelines for the use of animals in research of the Association for Research in Vision and Ophthalmology.

To determine the antitumor efficiency of Bel-sar treatment on pigmented and nonpigmented tumors, 1×10^5 B16F10 wild type or knock-out cells in 100 µl PBS were injected subcutaneously into the right flank of C57BL/6 mice. On day 9 after tumor inoculation, when the mean tumor size reached around 125 mm^3, mice were randomized into groups with similar-sized tumors. The hair surrounding the planned tumor treatment area was shaved off before Bel-sar treatment.

Mice were given 100 ug Bel-sar by intravenous (i.v.) injection, and 12 hours later, the tumors were treated with a 690 nm LED diode laser (CNI Laser) at a fluence rate of 400 mW/cm^2 for a total light dose (fluence) of 75 J/cm^2. Tumor volume and mouse weight were measured every 2 days. The tumor volume was calculated using the formula for cube (Length*Width*Height). The mice were euthanized when the tumor volume reached 1500 mm^3 or the body weight loss reached 15%.

We determined immune cell infiltration with and without treatment with light-activated Bel-sar in B16F10 wild type and TYR knock-out cell line-derived tumors. Tumors, spleen, and draining lymph nodes were harvested for flow cytometry analysis at day 11 (48 hours after PDT), and then single cell suspensions were collected as described before and stained with multiplexed monoclonal antibodies.[34] The antibodies that were used to stain the myeloid cell population were anti-CD45.2-APC-eFlour780 (clone HL3; Thermo Fisher), anti-CD11b-ef450 (clone M1/70; BD Biosciences), anti-CD11c-PE (clone N418; Thermo Fisher), anti-Ly6C-BV605 (clone HK1.4; Biolegend), ani-Ly6G-APC (clone

Investigative Ophthalmology & Visual Science

1A8; Biolegend), anti-F4/80-BV605 (clone BM8; Thermo Fisher), anti-CD86-BV785 (clone GL1; Thermo Fisher), anti-iNOS-AF488 and anti-CD206-BV421 (clone C068C2; Biolegend).

The antibodies that were used to stain the lymphoid cell population were: anti-CD45.2-APC-eFlour780 (clone 104; Thermo Fisher), anti-CD11c-APC (clone N418; Thermo Fisher), anti-CD3e-FITC (clone 17A2; Biolegend), anti-CD49b-PE, anti-CD4-BV711 (clone RM4-5; Biolegend), anti-CD8a-BV421 (clone 53-6.7; BD Bioscience), anti-IFN-r-PE-cy7 (clone B27; Biolegend), and anti-TNF-a-BV605 (clone MP6-XT22; Biolegend). Intracellular staining for iNOS, CD206, IFN-gamma, and TFN-alfa was performed according to the manufacturer's instructions. Analysis was performed using an Aurora cytometer (Cytek Biosciences).

Statistical Analysis

Statistical analyses were performed in GraphPad Prism version 9.0 for Windows (GraphPad Software). Unless otherwise stated, data are shown as the mean ± SEM of three independent experiments. Student's unpaired two-tailed *t*-test or one-way analysis of variance (ANOVA) were performed to compare two experimental groups. Statistical differences were considered significant at $^{*}P < 0.05$, $^{**}P < 0.01$, and $^{***}P < 0.001$.

Results

Loss of Visible Pigmentation and Melanosome Ultrastructure in TYR Knock-Out Cells

We visualized and compared the pigmentation of B16F10 wild type and TYR knock-out cells in a pellet after centrifugation and under light microscopy. The B16F10 wild type cell line gave rise to a highly pigmented pellet that was observed (Fig. 1A), whereas a light-grey color was produced by the TYR knock-out cells (Fig. 1B). Under light microscopy, the wild type cell line showed many heavily pigmented cells (Fig. 1C), whereas these were not present among the TYR knock-out cells (Fig. 1D), confirming the expected lack of pigmentation after TYR knock-out. During stage II melanosome formation, melanin is deposited in a melanosome. We analyzed the ultrastructure of melanosomes by transmission electron microscopy: in the wild type melanoma cells, different stages of melanosomes are visible, most larger mature melanosomes (reminiscent of stages III and IV; Fig. 1E), whereas the TYR knock-

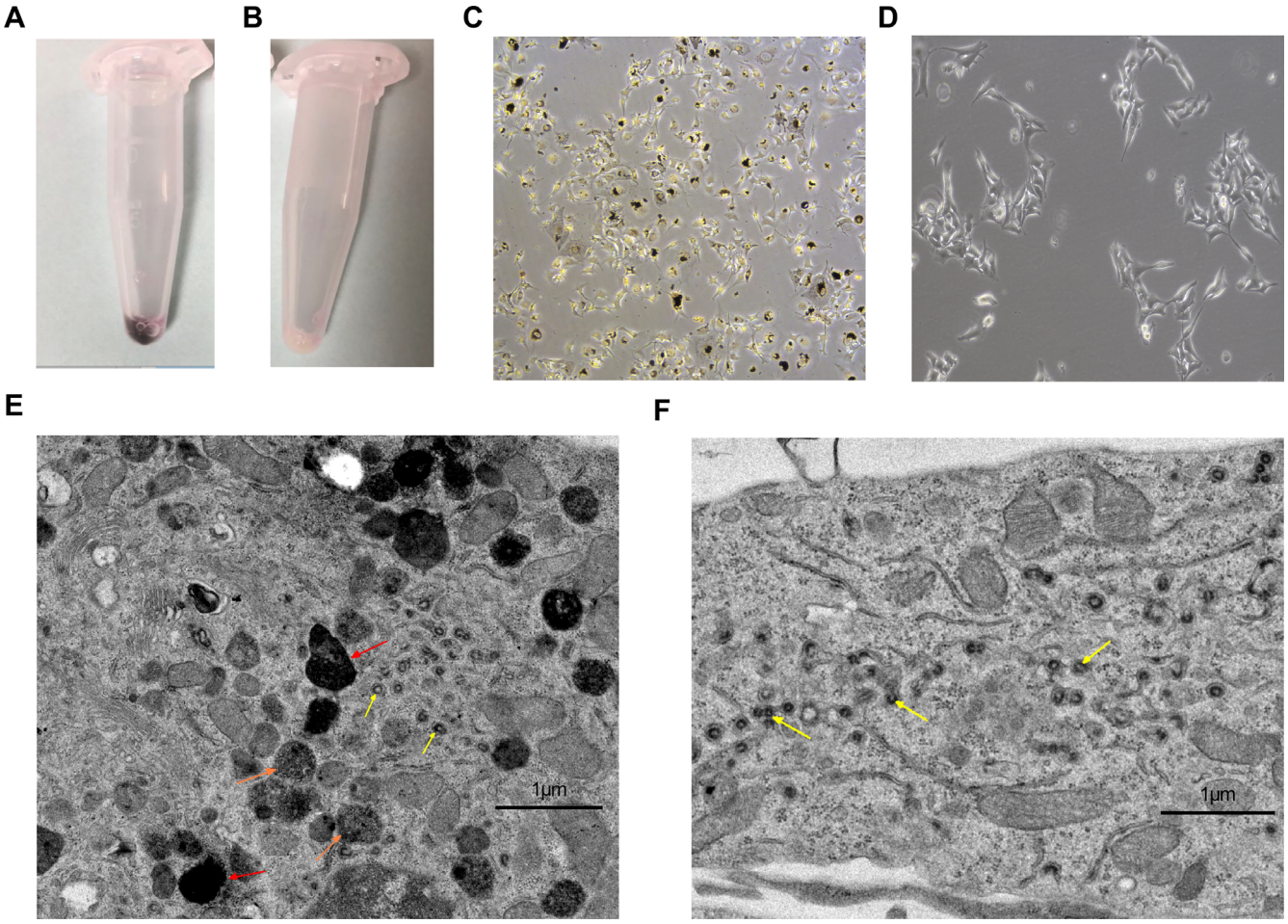

Figure 1. Loss of visible pigmentation and melanosome ultrastructure in B16F10 knock-out cells. (**A**, **B**) visible pigmentation of the pellet in wild type (**A**) but not in TYR knock-out cells (**B**). (**C**, **D**) heavily pigmented cells are visible in wild type (**C**) and not in cultured TYR knock-out cells (**D**) as seen by light microscopy (magnification 10 × 10 times). Transmission electron microscopy (magnification 6500 times) revealed (**E**) melanosomes at different stages (*yellow arrow* = stage I and stage II; *orange arrow* = stage III, and *red arrow* = stage IV melanosome) in the wild type cells (bar = 1 µm), but (**F**) only stage I and II melanosomes in the TYR knock-out cells (bar = 1 µm).

Investigative Ophthalmology & Visual Science

Table. Relative Expression of MDA Protein Expression in the Wild Type/TYR Knock-Out Cell Lines as Determined by Proteomic Analysis

	TYR	TYRP-1	TYRP-2	Gp-100	Melan-a	MITF
Ratio (wild type/knock-out)	10.75	1.08	1.16	0.94	1.36	0.80
***P* value**	0.02	0.23	0.12	0.11	0.06	0.02

Values represent the mean expression from three measurements.

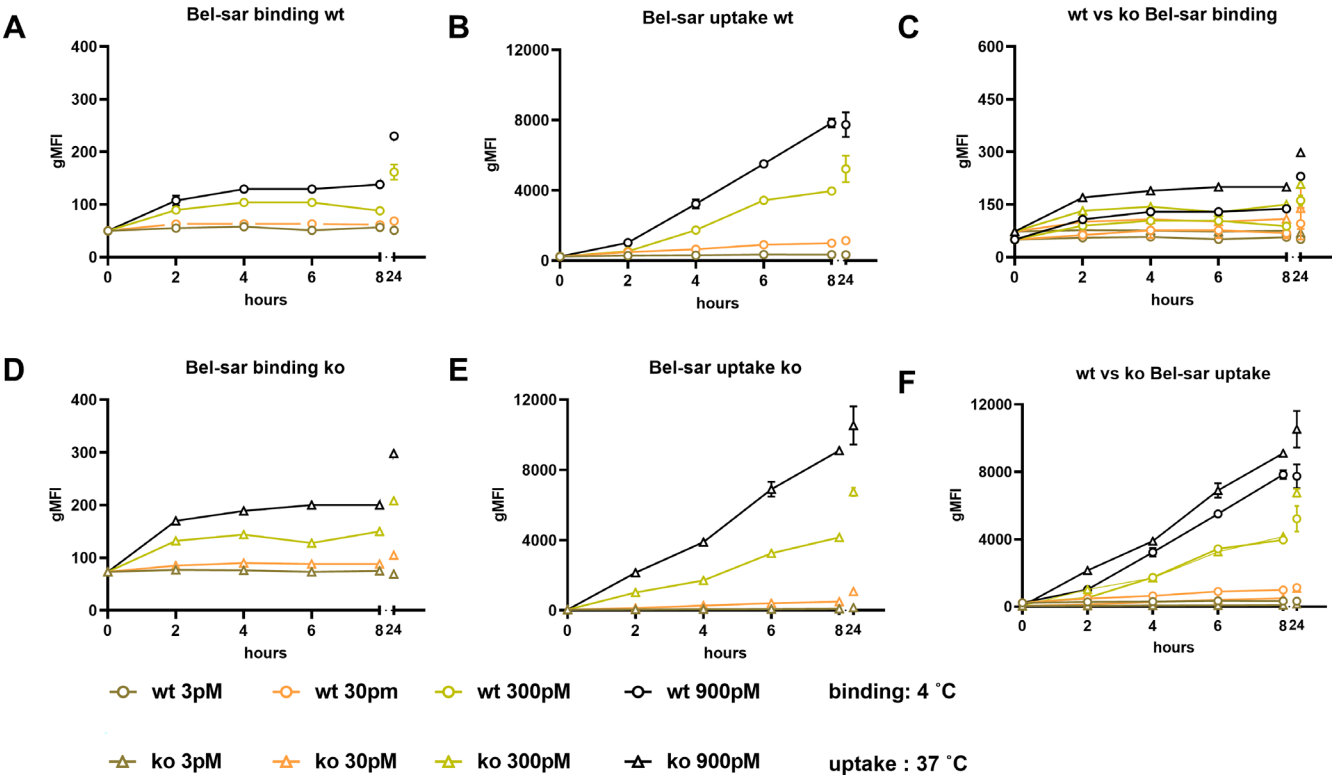

Figure 2. Binding and uptake of Bel-sar by B16F10 wild type and TYR knock-out cell line. (**A**, **D**) binding and (**B**, **E**) uptake kinetics of Bel-sar in B16F10 wild type and TYR knock-out cell lines at indicated concentration and incubation time, respectively. Comparing the binding (**C**) and uptake (**F**) of Bel-sar in B16F10 wild type and TYR knock-out cells, measured by FACS. Data are shown as the mean ± SEM of three independent experiments.

out cells only show larger fields of the smaller immature melanosomes (reminiscent of stages I and II; Fig. 1F). Knock-out of the tyrosinase gene produced a nonpigmented cell line with underdeveloped melanosomes.

Melanocyte Differentiation Antigen Expression: Proteomic Data

A wide range of melanocyte differentiation antigens (MDAs), such as TYRP-1, TYRP-2, gp-100, Melan-a, and MITF, are involved in the development and maturation of melanosomes. Therefore, we analyzed the relative expression of these proteins in wild type and TYR knock-out cells. As shown in the Table, the tyrosinase gene was not expressed in the TYR knock-out cells, whereas Melan-a was lower and MITF higher in the knock-out cells.

Cell Growth Behavior Between Pigmented and Non-Pigmented Cell Lines

We wondered whether the presence of melanin influenced tumor cell behavior, such as in vitro or in vivo tumor growth, or whether it influenced the response of the innate immune system against tumor cells. Cell growth (Supplementary Fig. S1A) showed no difference in in vitro proliferation between the two cell lines. We can conclude that knock-out of the tyrosinase gene led to amelanotic cells, which showed similar in vitro growth rates as their pigmented counterparts.

As pigmentation is considered a barrier for applying photodynamic treatment in melanoma, we compared the antitumor efficiency induced by Bel-sar treatment in the pigmented and nonpigmented cell lines in vitro and in vivo.

Intracellular Uptake of Bel-Sar

B16F10 wild type (Figs. 2A, 2B) and TYR knock-out (Figs. 2D, 2E) cells were incubated with different concentrations of Bel-sar, and uptake and binding were measured at different time points. At 37°C (uptake; see Figs. 2B, 2E), the gMFI was significantly higher than at 4°C (binding; see Figs. 2A, 2D), indicating that Bel-sar was effectively bound to the cell surface and the internalization into the cytoplasm was energy dependent. As the intensity of the signal did not differ significantly between the B16F10 wild

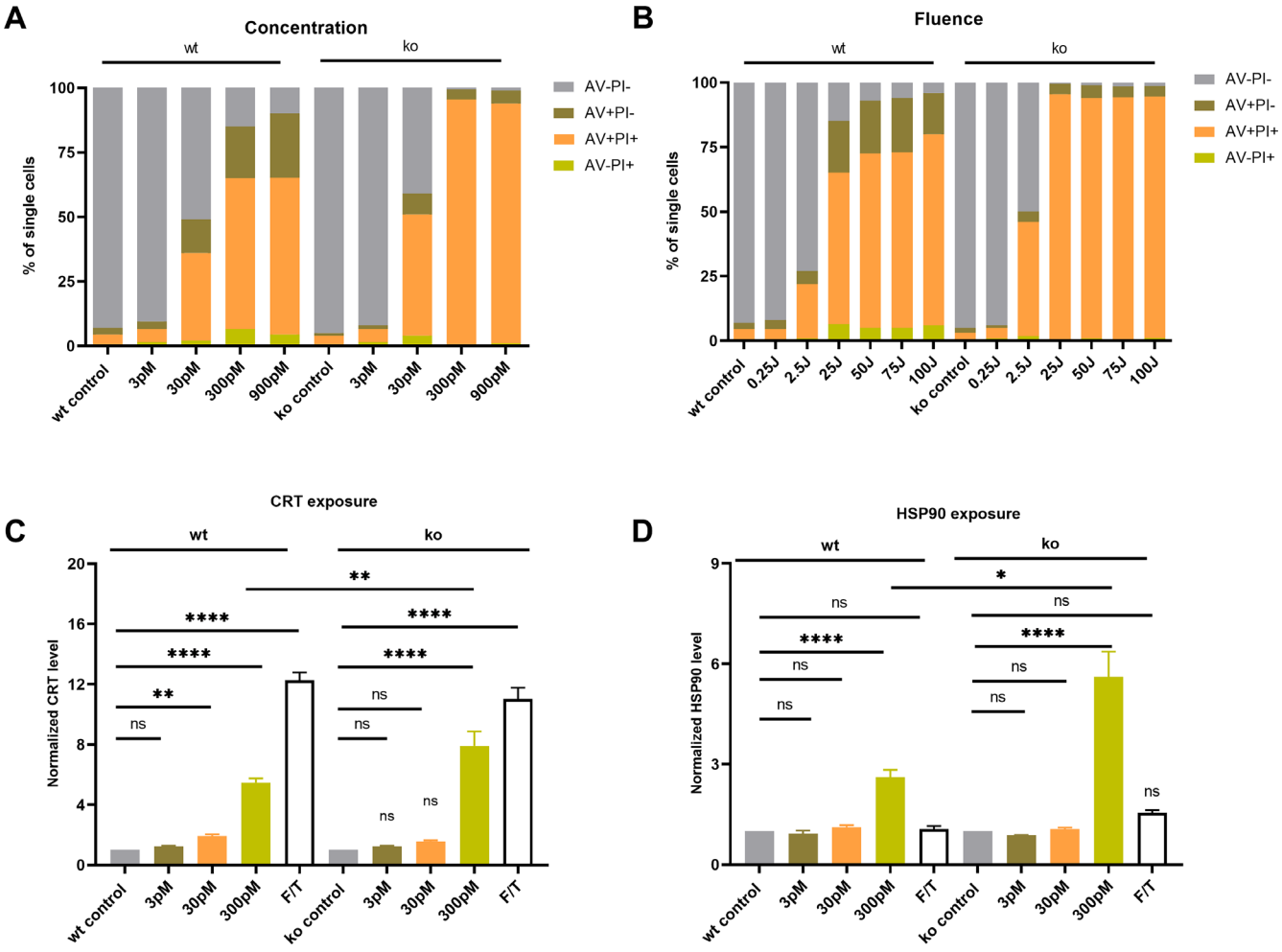

Figure 3. Cytotoxicity and cell surface exposure of CRT and HSP90 following Bel-sar treatment. The effect of (**A**) concentration and (**B**) fluence on in vitro cytotoxicity of Bel-sar treatment in B16F10 wild type and knock-out cells, measured by FACS after staining with Annexin V and PI. Annexin V staining indicates early apoptotic cells, whereas PI staining indicates late apoptotic cells. Increased levels of CRT (**C**) and HSP90 (**D**) on the cell surface as determined by FACS on B16F10 wild type and TYR knock-out cell lines on PI-negative cells. Tumor cells were treated with Bel-sar at the indicated concentrations followed by light activation or left untreated and analyzed 24 hours later. As a positive control, cells were frozen (−20°C) and thawed (37°C, F/T) three times. Data are shown as the mean ± SEM of three independent experiments and were statistically analyzed by an unpaired two-tailed Student's *t*-test. Statistical differences were considered significant at $^{*}P < 0.05$, $^{**}P < 0.01$, and $^{***}P < 0.001$.

type and knock-out cell line (see Figs. 2C, 2F), knock-out of the tyrosinase gene did not influence the binding and uptake of Bel-sar.

Cytotoxicity and Membrane Exposure of Damage Associated Molecular Pattern Molecules Induced by Light-Activated Bel-Sar

We set out to evaluate the effect of light-activated Bel-sar treatment on the pigmented and nonpigmented cell lines. The cytotoxicity induced by Bel-sar treatment was measured by determining the percentage of cells positive for PI or Annexin V (AV). PI-negative and AV-negative cells are considered alive, PI-negative AV+ cells are considered apoptotic, and PI + AV+ cells are considered dead. The Bel-sar concentration (pM) and fluence (total energy of irradiation, J/cm^2) were the main variables tested (Figs. 3A, 3B). The cytotoxicity of light-activated Bel-sar was enhanced with increasing concentrations of Bel-sar (see Fig. 3A) and with increasing fluence (see Fig. 3B). Light-activated Bel-sar treatment induced near complete cell death regardless of pigmentation. The half-maximal inhibitory concentration (IC_{50}) of the wild type cell and TYR knock-out cell line (see Supplementary Fig. S1B) did not differ significantly, indicating that the pigmentation level did not affect the cell viability of melanoma cells after Bel-sar treatment. The release or exposure of DAMPs that accompanies cell death may trigger an acute local inflammatory response which may then stimulate a systemic immune response. Two DAMPs are considered of particular importance for the immune response: CRT and HSP90. The effect of Bel-sar treatment on the exposure of CRT and HSP90 was measured by fluorescent activated cell sorting (FACS). The data show that CRT (Fig. 3C) and HSP90 (Fig. 3D) exposure were enhanced by Bel-sar treatment in both the pigmented as well as the nonpigmented tumor cells in a Bel-sar concentration-dependent manner. However, Bel-sar (at 300 pM) treatment induced a significantly higher CRT and HSP 90 exposure (see Figs. 3C, 3D) in the nonpigmented tumor cells

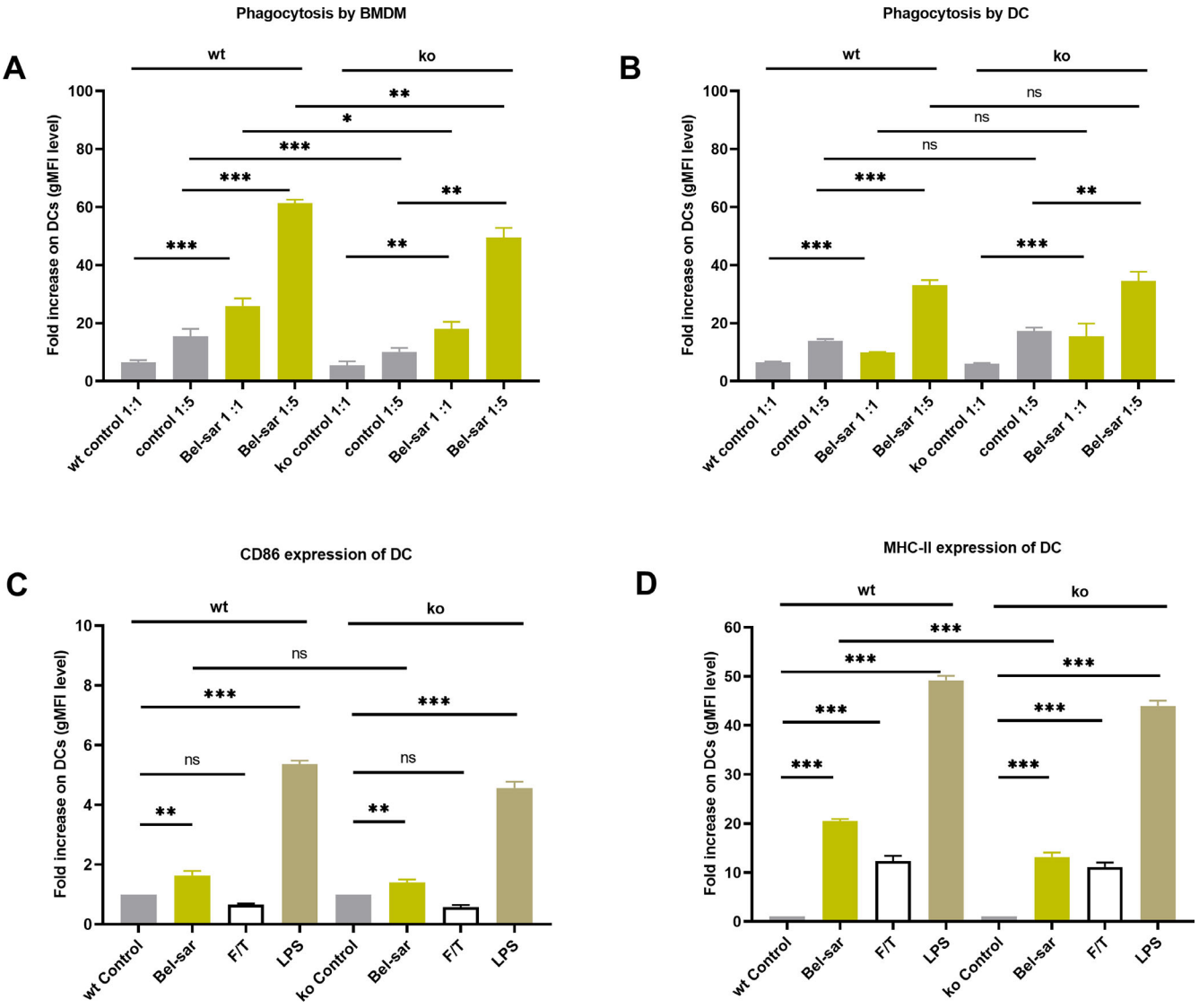

Figure 4. Phagocytosis of pigmented and nonpigmented melanoma cells was enhanced by Bel-sar treatment in vitro, and then increased the maturation markers on DCs. (**A**) After Bel-sar treatment, wild type and TYR knock-out melanoma cells were co-cultured in two different ratios (1:1 and 1:5) with BMDMs for 2 hours. Cell phagocytosis by BMDMs was scored as the percentage of CD11b+F4/80+CMFDA+ BMDMs (mean values ± SEM). (**B**) Following Bel-sar treatment, wild type and TYR knock-out melanoma cells were co-cultured with DCs at 2 different ratios (1:1 and 1:5) for 2 hours. Phagocytosis of DCs was scored as the percentage of CD11c+CMFDA+ DCs (mean values ± SEM). (**C**) Expression of CD86 and MHC-II (**D**) on DCs after co-culture with Bel-sar and laser treated B16F10 wild type and TYR knock-out melanoma cells, as measured by FACS. Freezing/thawing cells and LPS were used as positive controls. Data are shown as the mean ± SEM of three independent experiments and were statistically analyzed by an unpaired two-tailed Student's *t*-test. $^{*}P < 0.05$, $^{**}P < 0.01$, and $^{***}P < 0.001$.

compared with pigmented cells. We conclude that Bel-sar treatment increased DAMP exposure in pigmented as well as in nonpigmented melanoma cells, with a higher CRT and HSP90 exposure in the TYR knock-out cells under the treatment of 300 pM Bel-sar.

Light-Activated Bel-Sar Enhances Engulfment of Cancer Cells by Antigen Presenting Cells and Maturation of DCs

The exposure or release of DAMPs induced by Bel-sar treatment can work as a "find me" and "eat me" signal to antigen presenting cells (APCs), leading to engulfment of cells by these APCs. Typical APCs include macrophages, DCs, as well as B cells. In this study, we investigated the phagocytosis of BMDMs and DCs, and then the maturation of DCs.

To see whether Bel-sar treatment enhanced phagocytosis, we evaluated whether co-culture of BMDMs and DCs with Bel-sar treated cells enhanced phagocytosis compared to co-culture with untreated B16F10 cells. Pigmented wild type cells were more frequently engulfed by BMDMs (Fig. 4A) than nonpigmented TYR knock-out cells ($P < 0.05$), but pigmentation alone did not lead to a difference in phagocytosis by DCs (Fig. 4B). Pretreatment of melanoma cells (B16F10 wild type as well as TYR knock-out cells) with Bel-sar led to a more effective engulfment of cells by both murine BMDMs (see Fig. 4A) as well as DCs (see Fig. 4B).

As we noticed an increase in phagocytosis after Bel-sar treatment, we investigated the effect of the treat-

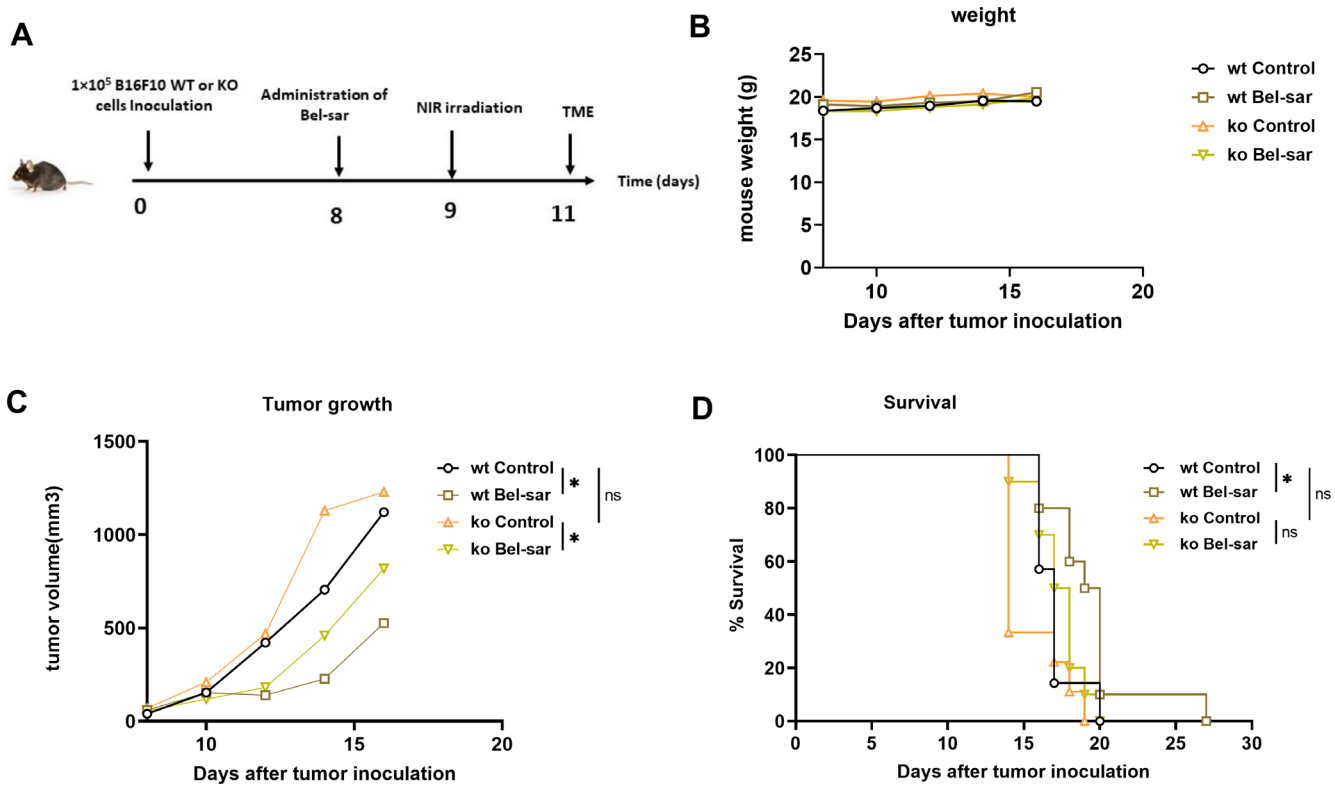

Figure 5. Bel-sar treatment induced tumor regression in wild type and knock-out tumors. (**A**) Schematic representation of the time course and regimen of administration for B16F10 wild type and TYR knock-out tumor-bearing mice (n = 7-11 in each group). (**B**) mouse weight after Bel-sar treatment and (**C**) changes in tumor size; (**D**) survival after Bel-sar treatment in wild type and TYR knock-out mice, displayed as the mean. For tumor growth and mouse weight, significance was determined using Student's t-tests. Significance in survival (n = 9–11 per group) was determined using the log-rank test. *$P < 0.05$, **$P < 0.01$, and ***$P < 0.001$.

ment on DC maturation: DCs undergo maturation after uptake of antigens, which will help to better present the processed antigens to T cells. We evaluated the expression of DC maturation markers CD86 and major histocompatibility complex (MHC) class II by FACS after 24 hours of co-culture wild type and TYR knock-out cells, with or without prior Bel-sar treatment. Co-culture of DCs with Bel-sar treated wild type and TYR knock-out cells led to enhanced CD86 (Fig. 4C) and MHC class II (Fig. 4D) expression on DCs. MHC class II expression was more upregulated after co-culturing with Bel-sar treated wild type than Bel-sar treated TYR knock-out cells (see Fig. 4D).

Bel-Sar Treatment-Induced Tumor Necrosis, Tumor Growth Inhibition, and Prolongation of Survival Are Independent of Pigmentation in a Subcutaneous B16F10 Tumor Model in Mice

We performed a series of in vivo experiments to investigate the role of pigmentation in Bel-sar treatment by comparing the antitumor effect on pigmented B16F10 wild type and nonpigmented B16F10 TYR knock-out tumors in a subcutaneous tumor model. At day 9 after tumor inoculation, tumors were treated by Bel-sar and laser following the schedule presented (Fig. 5A).

Two days after treatment, tumor necrosis was found in both the wild type (6/15, 40%) and TYR knock-out (3/14, 21%) tumors (Supplementary Table S1), a difference that was not statistically significant ($P = 0.68$). However, we observed more severe necrosis in the wild type tumors, compared with shallow and small necrotic areas in the TYR knock-out tumors (Supplementary Table S2). This difference approached statistical significance ($P = 0.07$). Overall, the wild type and TYR knock-out tumors showed a similar growth rate (see Fig. 5C) in the in vivo model, whereas Bel-sar treatment induced tumor regression in both models (see Fig. 5C) without inducing weight loss that might have indicated an off-target effect of the treatment (Fig. 5B). Bel-sar treatment decreased tumor growth in both models and prolonged survival of mice carrying a wild type tumor, although it did not significantly prolong survival in the TYR knock-out model (Fig. 5D). These data indicate that Bel-sar treatment can initiate tumor necrosis and tumor regression in both tumor models but leads to more necrosis when the lesions are pigmented.

The Tumor Microenvironment and Immune Response Induced by Light-Activated Bel-Sar Treatment in Pigmented and NonPigmented Tumors

From in vitro co-culture experiments, we already showed that Bel-sar treated pigmented tumor cells enhanced cell phagocytosis by BMDMs compared to the nonpigmented TYR knock-out cells. This led us to investigate whether Bel-

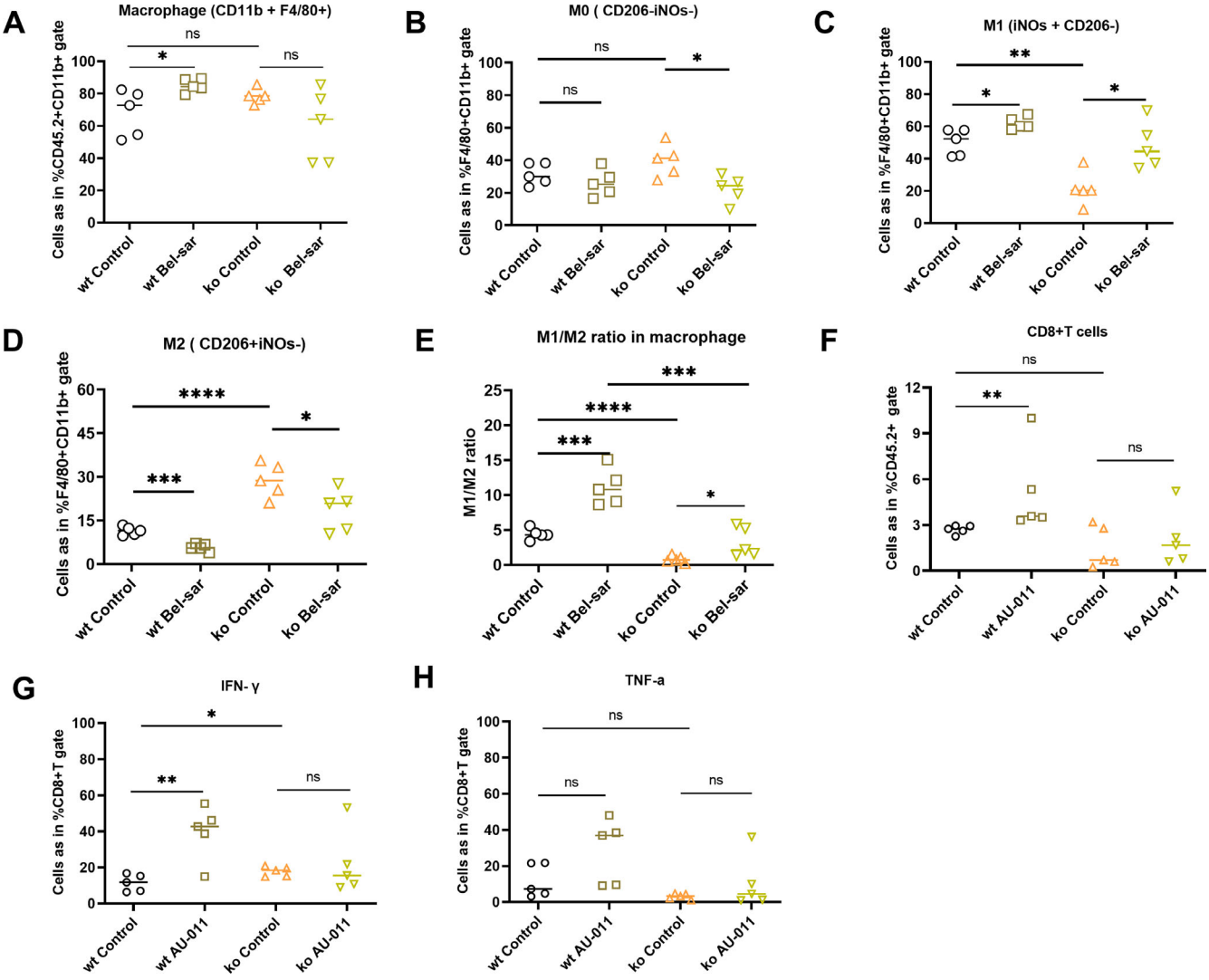

Figure 6. Macrophage and CD8+ T cell infiltration in wild type and TYR knock-out B16F10 tumors after Bel-sar treatment. Analysis of macrophages (**A**) CD11b+/F4/80+, M0 (**B**) iNOS-/CD206-, M1 (**C**) iNOS+/CD206-, M2 (**D**) iNOS-/ CD206+, M1/M2 ratio (**E**); and CD8+ T cells (**F**) CD45.2/CD3/CD8+, (**G**) IFN-gamma or (**H**) TNF-a positive CD8+ T cells in wild type and knock-out B16F10 tumors, with and without Bel-sar treatment. Statistical significance was determined using (multiple) Student's *t*-tests at various groups ($n = 5$ mice per group) $^{*}P < 0.05$, $^{**}P < 0.01$, and $^{***}P < 0.001$.

sar treatment induced either an innate or specific immune response, and whether the type or intensity of response might depend on the level of tumor pigmentation.

We set out to analyze the immunological tumor microenvironment in wild type and TYR knock-out tumors with and without Bel-sar treatment. At day 11 following Bel-sar treatment, the mice were euthanized and the type of immune cells was analyzed in the tumor, spleen, tumor-draining lymph node, and nontumor draining lymph node. Macrophages were the main immune infiltrating cells in treated as well as nontreated tumors. When looking at the untreated mice, the percentage of cells that were macrophages (CD11b+F4/80+) in the tumors did not differ in the wild type and TYR knock-out tumors (Fig. 6A). However, there was a difference in the type of infiltrating macrophages, with more M1 and less M2 macrophages in the wild type tumors compared to the TYR knock-out tumors (Figs. 6C, 6D), indicating that pigmentation may influence the type of infiltrating macrophage. Following light-activated Bel-sar treatment, the population of M2 macrophages was found to have relatively decreased, whereas the M1 population and M1/M2 ratio had increased in both the wild type and the TYR knock-out tumor model (see Figs. 6C, 6D, 6E), indicating that not only pigmentation but also Bel-sar treatment affects the macrophage polarization. When looking at T cell distribution, the untreated pigmented and nonpigmented tumors did not show a difference in CD3+, CD4+, or CD8+ T cells. However, after treatment with Bel-sar, we observed more CD8+ T cell and IFN-gamma positive CD8+ T cells in the wild type tumors than in the knock-out tumors (Figs. 6F, 6G). Analysis of the non-draining lymph nodes and of the spleen did not show differences between mice bearing wild type or TYR knock-out tumors, with or without Bel-sar treatment (data not shown). These data demonstrate an influence of pigmentation on macrophage polarization, with Bel-sar treatment leading to an influx of M1 macrophages and CD8+ T cells, independent of the tumor's pigmentation status.

Investigative Ophthalmology & Visual Science

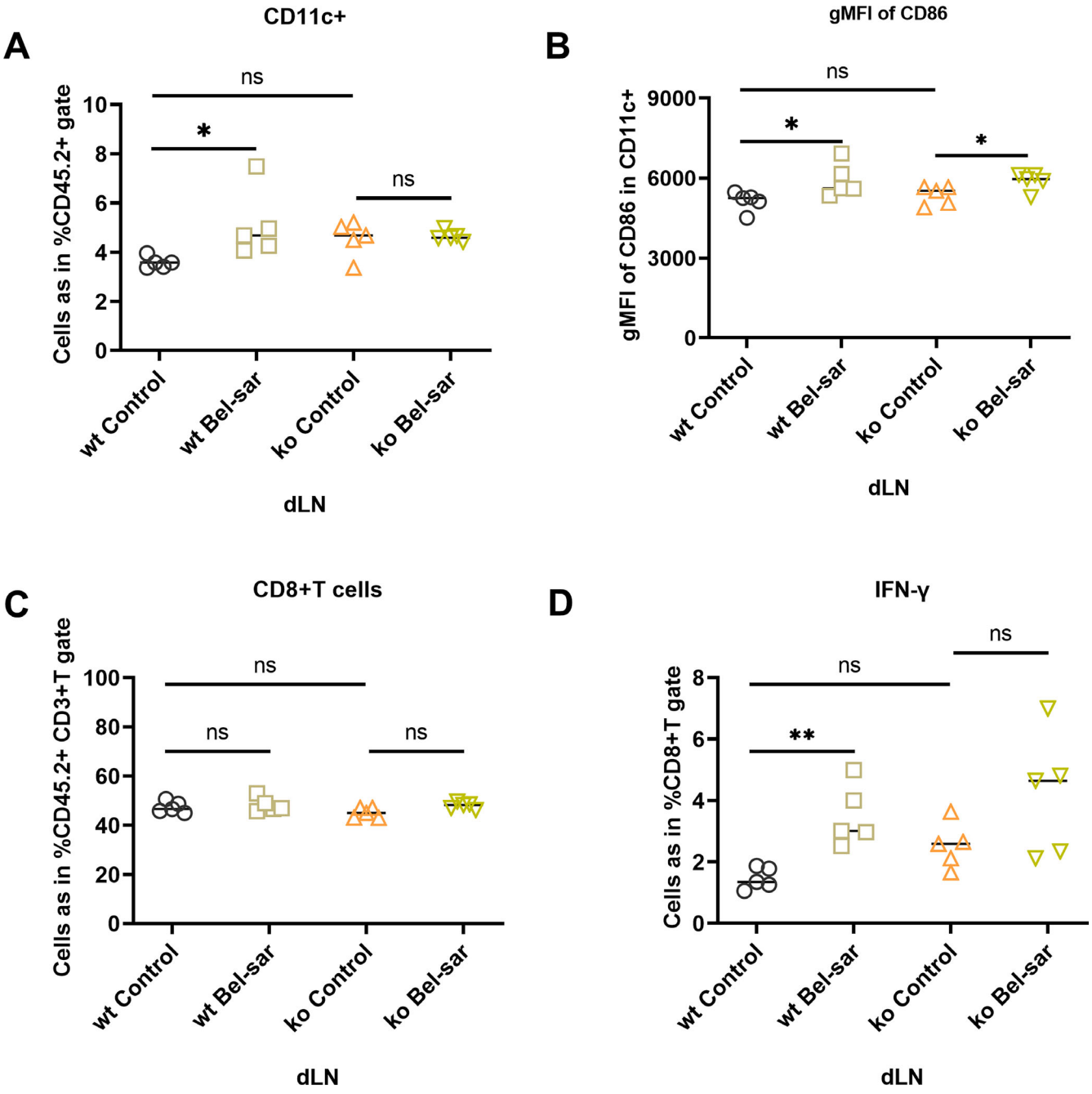

Figure 7. DC activation and CD8+T cell function in the DLN 11 days after light-activated Bel-sar treatment. Living (7AAD-) CD45.2 cells were further gated into DCs (CD11c+), CD3+T cells, CD8+ T cells (CD3+CD8+), and CD8+/IFN g+ cells. (**A**) Analysis of the presence of DCs (CD45.2+/CD11c+). (**B**) Presence of DC maturation marker CD86 on DCs (CD45.2+/CD11c+/CD86+). (**C**) Presence of CD8+ T cells among CD45.2+ CD3+ T cells, or (**D**) IFN-gamma positive CD8+ T cells among CD45.2+ cells in draining lymph nodes. The graphs show the mean gMFI ± SEM of CD86 on DCs to indicate their activation. Statistical significance was determined using (multiple) Student's *t*-tests at various group ($n = 5$ mice per group) $^{*}P < 0.05$, $^{**}P < 0.01$, and $^{***}P < 0.001$.

Our in vitro data had shown that Bel-sar treated tumor cells enhanced the maturation of DCs. We set out to analyze the presence of DCs and CD8+ T cells and their activation state in the tumor draining lymph node, comparing mice bearing B16F10 wild type and knock-out tumors, and with and without light-activated Bel-sar treatment. No difference was observed in the analyzed cell types in the draining lymph node between untreated mice with B16F10 wild type or TYR knock-out tumors. After Bel-sar treatment, an increase in the number of CD11c+ DCs was observed in the draining lymph nodes in B16F10 wild type tumors but not in B16F10 knock-out tumors. Furthermore, a significant increase was present in CD86+ DCs in both the B16F10 wild type and knock-out tumor-bearing mice (Figs. 7A, 7B). Light-activated Bel-sar treatment enhanced the number of IFN-gamma positive CD8+ T cells without inducing more CD8+ T cells in the mice with wild type B16F10 tumors (Figs. 7C, 7D). In the mice bearing a TYR knock-out tumor,

Investigative Ophthalmology & Visual Science

a large variation in the interferon-gamma response was seen. Bel-sar treatment enhanced the CD8+T cell function only in the wild type draining lymph nodes, but not in the knock-out draining lymph nodes. Our findings suggest that light-activated Bel-sar treatment induces inflammation in the wild type as well as TYR knock-out tumor model, and stimulates lymphocyte infiltration in the tumor microenvironment, polarizes M2 macrophages to become M1 macrophages, and leads to activation of DCs and CD8+ T cells in the draining lymph nodes.

We can conclude that knock-out of TYR led to reduced pigmentation with cells carrying immature melanosomes. Nonpigmented cells showed the same proliferation rate in vitro as the pigmented cells. Pigmented cells were better at stimulating phagocytosis by BMDMs but not by DCs, and the pigmented tumors contained relatively more M1 macrophages. There was no significant growth difference in the development of pigmented versus nonpigmented subcutaneous tumors. Treatment with light-activated Bel-sar killed nonpigmented as well as pigmented cells in vitro and led to necrosis (more in pigmented tumors) and growth inhibition in both models in vivo. The Bel-sar treatment induced DAMP exposure and activation of DCs, and a shift toward more M1 macrophages in the tumor in vivo, which was more prominent in pigmented tumors. Treatment with Bel-sar also led to higher numbers of IFN-gamma positive CD8 cells in the tumors and draining lymph nodes of pigmented tumors as well as increased numbers of CD11c+ DCs in the same draining lymph nodes. The Bel-sar stimulated the presence of CD86+ DCs in the draining lymph nodes of both the pigmented as well as the nonpigmented tumors.

Discussion

We investigated the role of pigmentation in tumor behavior and compared the antitumor efficiency of Bel-sar treatment in pigmented and nonpigmented melanoma cells in vitro and in vivo. We demonstrated that pigmentation does not affect cell or tumor growth in vitro and in vivo but influences phagocytosis and the type of infiltrating macrophage in the tumors, leading to more M1 macrophage infiltration in pigmented tumors. We then determined the effect of light-activated Bel-sar treatment on the pigmented and nonpigmented cells in vitro and in a subcutaneous tumor model, using a wild type and TYR knock-out cell line. Clinical evidence in UM has shown that pigmentation increased the resistance to the radiotherapy, indicating that melanogenesis could be a possible target for melanoma therapy.[35] Melanin has been described as a factor that increases cell resistance to PDT, and functions as an intrinsic defense system against oxidants. We previously tested a series of 10 human UM cell lines, and observed that all were susceptible to killing using light-activated Bel-sar, although at different sensitivities.[36] Such cell lines vary in many different aspects, and could not provide an answer to the question whether pigmentation influenced treatment. We therefore used the TYR wild type and knock-out B16F10 models, and show that pigmentation does not provide a barrier for applying the light-activated Bel-sar treatment in these melanomas: Bel-sar treatment induced near complete cell death in vitro, accompanied by immunogenic cell death as shown by DAMP exposure and by activation of APCs, and effectively delayed tumor growth in the pigmented as well as in the non-pigmented in vivo model, while stimulating macrophage M1 influx.

We should furthermore consider that, in this paper, we used the murine B16F10 cutaneous model to investigate the role of pigmentation in the tumor microenvironment and antitumor efficiency of Bel-sar. However, the immune privilege of the eye may influence the induction or effect of the immune response caused by Bel-sar treatment. The immune privilege of the eye is characterized by the downregulation of delayed-type hypersensitivity responses, through interactions among antigen-presenting cells, T cells, and intraocular fluids. This means that the immune infiltrate may differ between the intraocular and subcutaneous tumor model, and that T-cell responses may be less effective.[37,38] We do not know how the eye's immune characteristics would influence macrophage influx. Further preclinical and clinical studies should be performed to investigate this issue.

In our data, pigmentation contributed to increased phagocytosis by BMDMs in vitro, whereas in the in vivo model, pigmented tumors contained more M1 and fewer M2 macrophages compared to nonpigmented tumors. We were surprised to see this, as in human UM, increased pigmentation and the presence of higher numbers of M2 macrophages are associated, and related to the same genetic factor, chromosome 3/BAP1 loss.[3,21,39,40] Tumors with BAP1/chromosome 3 loss often have an inflammatory phenotype and show a typical mRNA profile known as class 2.[41–43] It is characterized by an increased presence of infiltrating T cells and macrophages, especially M2 type macrophages.[21,22] It is therefore very interesting that, in our mouse model, pigmented tumors contained more M1 macrophages. This may be related to the age of the mice, as prior experiments from our laboratory showed that young and old mice carry different types of macrophages in intraocular tumors.[44] Depletion of macrophages would stop tumor growth in 2-year-old mice, but not in young mice, suggesting that tumors in old mice were mainly tumor-inducing M2 macrophages.

In the current experiments, treatment with Bel-sar changed the balance between M1 and M2 macrophages toward M1, which may help in stimulating antitumor immune responses. In addition, Bel-sar treatment induced an increase in IFN-gamma positive CD8 cells in the tumor as well as the draining lymph nodes, but this was mainly seen in mice with wild type tumors.

There are limited data on how pigmentation affects TME in in vivo models, but more is known about how melanogenesis might promote an immunosuppressive microenvironment in in vitro co-culture experiments.[45] The synthetic melanin of CM could suppress the production of proinflammatory cytokines by immune cells.[46,47] In a co-culture experiment, melanoma cells were incubated with PBMCs, which induced production of cytokines, such as IL-1beta, IL-2, IL-6, and IL-12. Chemical inhibition of melanogenesis in the melanoma cells led to an increase or decrease in production of proinflammatory cytokines by PBMC.[47] More interestingly, melanin could serve as a target for an adjuvant therapy to enhance the sensitivity of melanoma to immunity therapy.[48–50] The melanosome is a lysosome related organelle and its membrane is considered as a part of endosomal membrane, which can be targeted by photosensitizer.[51,52] Melanocyte differentiation antigens are not just involved in the maturation of melanosomes, but are important antigens of UM and CM even though they are derived from nonmutated "self" proteins. The results of treating UM metastases with tebentafusp, a bispecific antibody that binds T cells as well as gp100, show the importance of gp100 as a tumor

Investigative Ophthalmology & Visual Science

antigen.[53] Other melanocyte differentiation antigens, such as TRP1, TRP2, and MART1, could also induce immune response in melanoma.[54–56] PDT by itself can enhance the exposure or release of tumor associated antigens (TAAs), as shown by an increase in the number of tumor specific CD8+ T cells.[16]

In the clinic, verteporfin has been used to treat small choroidal melanoma. In one study, 53 out of 83 pigmented tumors showed complete or partial regression, whereas all 69 nonpigmented tumors showed complete regression.[9] This makes it attractive to look for a photosensitizer that can treat pigmented tumors as well. Light-activated Bel-sar induced near complete cell death in vitro and delayed tumor growth in our in vitro as well as our in vivo model, regardless of pigmentation. These data indicate that Bel-sar treatment could be an ideal candidate to treat both pigmented and nonpigmented UM in the clinic. This may be attributable to the unique characteristic of Bel-sar: first, a single virus-like particle (VLP) is conjugated to a large number of phthalocyanine photosensitizer molecules, and this leads to the high accumulation of photosensitizer on the cell membrane and intracellularly. Our binding and uptake data confirmed prior findings. Second, the VLP specifically targets the membrane on tumor cells by HSPGs; Third, the included photosensitizer is activated at a wavelength of a 690 nm laser which can penetrate deep tissues.[26,28] The high accumulation of the Bel-sar in the tumor and deep penetration of laser overcomes the barrier of pigmentation. The limited regression after verteporfin treatment may be due to the characteristics of verteporfin PDT. Verteporfin PDT mainly targets blood vessels due to the short time between the administration of the photosensitizer and irradiation. After a short incubation time, verteporfin did not induce the exposure or release of DAMPs in vitro.[57]

Our data show that Bel-sar treatment induced immunogenetic cell death, characterized by increased exposure of DAMPs and activation of APCs regardless of pigmentation. DAMPs, including HSP 90 and CRT, are indicators of immunogenic cell death due to the ability to interact with APCs or other immune cells.[12–14] DC maturation is a pivotal induction step of the immune response.[58] In this study, we show that Bel-sar treated tumor cells can be phagocytosed by BMDMs or DCs and subsequently induce maturation of DCs in vitro, as shown by the increased expression of CD86 and MHC class II, which is consistent with the concept that PDT treated cells are immunogenic.[59–61] The infiltration with specific M2 type macrophages is associated with shorter time to death resulting from metastasis in UMs.[19] M2-type macrophages have the potential to enhance angiogenesis, induce immune suppression, and are associated with metastasis formation.[18] Repolarization of the tumor associated macrophages may also be one of the mechanisms of action of Bel-sar treatment, which can be a potential combination strategy. Repolarization of M2 type macrophage also contributes to the tumor ablation triggered by PDT.[57]

In agreement with the in vitro results, Bel-sar treatment delays tumor outgrowth in both models and induced maturation of DCs as shown in tumor-draining lymph nodes; however, it only enhanced the function of CD8+ T cells in pigmented tumors and their draining lymph nodes. The presence of pigment led to the different T cell response to Bel-sar treatment in pigmented and nonpigmented model. Notably, treatment with PDT only did not induce complete tumor ablation. However, UM has the high risk to develop metastasis in the clinic when the tumor size is larger than 3 mm.[62] The combination with other therapies, such as immune check point inhibitors, may be necessary to induce the complete tumor ablation and stronger systemic immune response to prevent UM metastasis in the clinic. The International Classification of Diseases (ICD) and favorable microenvironment triggered by Bel-sar treatment are indicators for combination with immune check point inhibitors to induce the local and distant tumor cure.[16,17,63] Further preclinical and clinical studies to investigate the combination Bel-sar treatment and immune checkpoint inhibitors should be conducted. Our results indicate that despite the light-absorbing function of pigments, which was proposed to be detrimental for laser therapy, we could show that Bel-sar treatment can enhance antitumor immune effects even in pigmented malignancies.

Acknowledgments

The authors especially thank Roman Koning and Carolina Jost from the electron microscopy facility, and Rayman T.N. Tjokrodirijo from the Center of Proteomics and Metabolomics at the LUMC for the discussion.

Supported by a grant from the China Scholarship Council to S.M. and a Health Holland grant to M.J.J.

Disclosure: **S. Ma**, None; **R.V. Huis in't Veld**, None; **Y. Hao**, None; **Z. Gu**, None; **C. Rich**, (C); **M.C. Gelmi**, None; **A.A. Mulder**, None; **P.A. van Veelen**, None; **T.K.H. Vu**, None; **T. van Hall**, None; **F.A. Ossendorp**, None; **M.J. Jager**, None

References

1. Virgili G, Gatta G, Ciccolallo L, et al. Incidence of uveal melanoma in Europe. *Ophthalmology*. 2007;114(12):2309–2315.
2. Jager MJ, Shields CL, Cebulla CM, et al. Uveal melanoma. *Nat Rev Dis Primers*. 2020;6(1):24.
3. Gelmi MC, Wierenga AP, Kroes WG, et al. Increased histological tumor pigmentation in uveal melanoma is related to eye color and loss of chromosome 3/BAP1. *Ophthalmol Sci*. 2023;3(3):100297.
4. Huang YY, Vecchio D, Avci P, et al. Melanoma resistance to photodynamic therapy: new insights. *J Biol Chem*. 2013;394(2):239–250.
5. Turkoglu EB, Pointdujour-Lim R, Mashayekhi A, Shields CL. Photodynamic therapy as primary treatment for small choroidal melanoma. *Retina*. 2019;39(7):1319–1325.
6. Sealy RC, Sarna T, Wanner EJ, Reszka K. Photosensitization of melanin: an electron spin resonance study of sensitized radical production and oxygen consumption. *Photochem Photobiol*. 1984;40(4):453–459.
7. Tada M, Kohno M, Niwano Y. Scavenging or quenching effect of melanin on superoxide anion and singlet oxygen. *J Clin Biochem Nutr*. 2010;46(3):224–228.
8. Sheleg SV, Zhavrid EA, Khodina TV, et al. Photodynamic therapy with chlorin e(6) for skin metastases of melanoma. *Photodermatol Photoimmunol Photomed*. 2004;20(1):21–26.
9. Yordi S, Soto H, Bowen RC, Singh AD. Photodynamic therapy for choroidal melanoma: what is the response rate? *Surv Ophthalmol*. 2021;66(4):552–559.
10. Van Straten D, Mashayekhi V, De Bruijn HS, et al. Oncologic photodynamic therapy: basic principles, current clinical status and future directions. *Cancers*. 2017;9(2):19.
11. Huis In 't Veld RV, Heuts J, Ma S, et al. Current challenges and opportunities of photodynamic therapy against cancer. *Pharmaceutics*. 2023;15(2):330.

12. Garg AD, Agostinis P. ER stress, autophagy and immunogenic cell death in photodynamic therapy-induced anticancer immune responses. *Photochem Photobiol Sci*. 2014;13(3):474–487.
13. Krysko DV, Garg AD, Kaczmarek A, et al. Immunogenic cell death and DAMPs in cancer therapy. *Nat Rev Cancer*. 2012;12(12):860–875.
14. Obeid M, Tesniere A, Ghiringhelli F, et al. Calreticulin exposure dictates the immunogenicity of cancer cell death. *Nat Med*. 2007;13(1):54–61.
15. Hickman-Miller HD, Hildebrand WH. The immune response under stress: the role of HSP-derived peptides. *Trends Immunol*. 2004;25(8):427–433.
16. Kleinovink JW, Fransen MF, Lowik CW, Ossendorp F. Photodynamic-immune checkpoint therapy eradicates local and distant tumors by CD8(+) T cells. *Cancer Immunol Res*. 2017;5(10):832–838.
17. Huis In't Veld RV, Ma S, Kines RC, et al. Immune checkpoint inhibition combined with targeted therapy using a novel virus-like drug conjugate induces complete responses in a murine model of local and distant tumors. *Cancer Immunol Immunother*. 2023;72(7):2405–2422.
18. Mantovani A, Allavena P, Marchesi F, Garlanda C. Macrophages as tools and targets in cancer therapy. *Nat Rev Drug Discov*. 2022;21(11):799–820.
19. Makitie T, Summanen P, Tarkkanen A, Kivela T. Tumor-infiltrating macrophages (CD68(+) cells) and prognosis in malignant uveal melanoma. *Invest Ophthalmol Vis Sci*. 2001;42(7):1414–1421.
20. Toivonen P, Makitie T, Kujala E, Kivela T. Microcirculation and tumor-infiltrating macrophages in choroidal and ciliary body melanoma and corresponding metastases. *Invest Ophthalmol Vis Sci*. 2004;45(1):1–6.
21. Maat W, Ly LV, Jordanova ES, et al. Monosomy of chromosome 3 and an inflammatory phenotype occur together in uveal melanoma. *Invest Ophthalmol Vis Sci*. 2008;49(2):505–510.
22. Bronkhorst IHG, Ly LV, Jordanova ES, et al. Detection of M2-macrophages in uveal melanoma and relation with survival. *Invest Ophthalmol Vis Sci*. 2011;52(2):643–650.
23. Christofides A, Strauss L, Yeo A, et al. The complex role of tumor-infiltrating macrophages. *Nat Immunol*. 2022;23(8):1148–1156.
24. Gezgin G, Visser M, Ruano D, et al. Tumor-infiltrating T cells can be expanded successfully from primary uveal melanoma after separation from their tumor environment. *Ophthalmol Sci*. 2022;2(2):100132.
25. Streilein JW. Ocular immune privilege: therapeutic opportunities from an experiment of nature. *Nat Rev Immunol*. 2003;3(11):879–889.
26. Kines RC, Varsavsky I, Choudhary S, et al. An infrared dye-conjugated virus-like particle for the treatment of primary uveal melanoma. *Mol Cancer Ther*. 2018;17(2):565–574.
27. Kines RC, Thompson CD, Spring S, et al. Virus-like particle-drug conjugates induce protective, long-lasting adaptive antitumor immunity in the absence of specifically targeted tumor antigens. *Cancer Immunol Res*. 2021;9(6):693–706.
28. Kines RC, Schiller JT. Harnessing human papillomavirus' natural tropism to target tumors. *Viruses*. 2022;14(8):1656.
29. Benito-Martinez S, Zhu YY, Jani RA, et al. Research techniques made simple: cell biology methods for the analysis of pigmentation. *J Invest Dermatol*. 2020;140(2):257–268.
30. Faas FGA, Avramut MC, van den Berg BM, et al. Virtual nanoscopy: generation of ultra-large high resolution electron microscopy maps. *J Cell Biol*. 2012;198(3):457–469.
31. van de Kooij B, de Vries E, Rooswinkel RW, et al. N-terminal acetylation can stabilize proteins independent of their ubiquitination. *Sci Rep*. 2023;13(1):5333.
32. van Dinten LC, Pul N, van Nieuwpoort AF, et al. Uveal and cutaneous melanoma: shared expression characteristics of melanoma-associated antigens. *Invest Ophthalmol Vis Sci*. 2005;46(1):24–30.
33. Toda G, Yamauchi T, Kadowaki T, Ueki K. Preparation and culture of bone marrow-derived macrophages from mice for functional analysis. *STAR Protoc*. 2021;2(1):100246.
34. Kleinovink JW, Ossendorp F. Measuring the antitumor T-cell response in the context of photodynamic therapy. *Methods Mol Biol*. 2022;2451:579–588.
35. Brozyna AA, VanMiddlesworth L, Slominski AT. Inhibition of melanogenesis as a radiation sensitizer for melanoma therapy. *Int J Cancer*. 2008;123(6):1448–1456.
36. Ma S, Huis In't Veld RV, Houy A, et al. In vitro testing of the virus-like drug conjugate belzupacap sarotalocan (AU-011) on uveal melanoma suggests BAP1-related immunostimulatory capacity. *Invest Ophthalmol Vis Sci*. 2023;64(7):10.
37. Wilbanks GA, Mammolenti M, Streilein JW. Studies on the induction of anterior chamber-associated immune deviation (Acaid). 3. Induction of Acaid depends upon intraocular transforming growth-factor-Beta. *Eur J Immunol*. 1992;22(1):165–173.
38. Streilein JW. Ocular immune privilege: the eye takes a dim but practical view of immunity and inflammation. *J Leukoc Biol*. 2003;74(2):179–185.
39. Figueiredo CR, Kalirai H, Sacco JJ, et al. Loss of BAP1 expression is associated with an immunosuppressive microenvironment in uveal melanoma, with implications for immunotherapy development. *J Pathol*. 2020;250(4):420–439.
40. Wierenga APA, Brouwer NJ, Gelmi MC, et al. Chromosome 3 and 8q aberrations in uveal melanoma show greater impact on survival in patients with light iris versus dark iris color. *Ophthalmology*. 2022;129(4):421–430.
41. Onken MD, Worley LA, Ehlers JP, Harbour JW. Gene expression profiling in uveal melanoma reveals two molecular classes and predicts metastatic death. *Cancer Res*. 2004;64(20):7205–7209.
42. van Essen TH, van Pelt SI, Versluis M, et al. Prognostic parameters in uveal melanoma and their association with BAP1 expression. *Br J Ophthalmol*. 2014;98(12):1738–1743.
43. Robertson AG, Shih JL, Yau C, et al. Integrative analysis identifies four molecular and clinical subsets in uveal melanoma (vol 32, pg 204, 2017). *Cancer Cell*. 2018;33(1):151.
44. Ly LV, Baghat A, Versluis M, et al. Aged mice, outgrowth of intraocular melanoma depends on proangiogenic M2-type macrophages. *J Immunol*. 2010;185(6):3481–3488.
45. Cabaço LC, Tomás A, Pojo M, Barral DC. The dark side of melanin secretion in cutaneous melanoma aggressiveness. *Front Oncol*. 2022;12:887366.
46. Mohagheghpour N, Waleh N, Garger SJ, et al. Synthetic melanin suppresses production of proinflammatory cytokines. *Cell Immunol*. 2000;199(1):25–36.
47. Pawlikowska M, Jędrzejewski T, Slominski AT, et al. Pigmentation levels affect melanoma responses to coriolus versicolor extract and play a crucial role in melanoma-mononuclear cell crosstalk. *Int J Molec Sci*. 2021;22(11):5735.
48. Ye YQ, Wang C, Zhang XD, et al. A melanin-mediated cancer immunotherapy patch. *Sci Immunol*. 2017;2(17):eaan5692.
49. Cuzzubbo S, Roch B, Darrasse-Jèze G, et al. Synthetic melanin acts as efficient peptide carrier in cancer vaccine strategy. *Int J Molec Sci*. 2022;23(23):14975.
50. Carpentier AF, Geinguenaud F, Tran T, et al. Synthetic melanin bound to subunit vaccine antigens significantly enhances CD8+ T-cell responses. *PLoS One*. 2017;12(7):e0181403.

Investigative Ophthalmology & Visual Science

51. Raposo G, Marks MS. Melanosomes-dark organelles enlighten endosomal membrane transport. *Nat Rev Molec Cell Biol*. 2007;8(10):786–797.
52. Valli F, Vior MCG, Riega SDE, et al. Melanosomal targeting via caveolin-1 dependent endocytosis mediates ZN (II) phthalocyanine phototoxic action in melanoma cells. *J Photochem Photobiol B*. 2022;234:112505.
53. Carvajal RD, Butler MO, Shoushtari AN, et al. Clinical and molecular response to tebentafusp in previously treated patients with metastatic uveal melanoma: a phase 2 trial. *Nat Med*. 2022;28(11):2364–2373.
54. Bloom MB, PerryLalley D, Robbins PF, et al. Identification of tyrosinase-related protein 2 as a tumor rejection antigen for the B16 melanoma. *J Exp Med*. 1997;185(3):453–459.
55. Castle JC, Kreiter S, Diekmann J, et al. Exploiting the mutanome for tumor vaccination. *Cancer Res*. 2012;72(5):1081–1091.
56. Kreiter S, Vormehr M, van de Roemer N, et al. Mutant MHC class II epitopes drive therapeutic immune responses to cancer. *Nature*. 2015;520(7549):692–696.
57. Hao Y, Ma S, Gu Z, et al. Combination of photodynamic therapy and stimulator of interferon genes (STING) agonist inhibits colorectal tumor growth and recurrence. *Cancer Commun*. 2023;43(4):513.
58. Murphy TL, Murphy KM. Dendritic cells in cancer immunology. *Cell Mol Immunol*. 2022;19(1):3–13.
59. Alzeibak R, Mishchenko TA, Shilyagina NY. Targeting immunogenic cancer cell death by photodynamic therapy: past, present and future (vol 9, e001926, 2021). *J Immunother Cancer*. 2021;9(10):e001926.
60. Turubanova VD, Balalaeva IV, Mishchenko TA, et al. Immunogenic cell death induced by a new photodynamic therapy based on photosens and photodithazine. *J Immunother Cancer*. 2019;7(1):1–13.
61. Tanaka M, Kataoka H, Yano S, et al. Immunogenic cell death due to a new photodynamic therapy (PDT) with glycoconjugated chlorin (G-chlorin). *Oncotarget*. 2016;7(30):47242–47251.
62. Jouhi S, Jager MJ, Geus SJR, et al. The small fatal choroidal melanoma study. A survey by the European Ophthalmic Oncology Group. *Am J Ophthalmol*. 2019;202:100–108.
63. Kim S, Kim SA, Nam GH, et al. In situ immunogenic clearance induced by a combination of photodynamic therapy and rho-kinase inhibition sensitizes immune checkpoint blockade response to elicit systemic antitumor immunity against intraocular melanoma and its metastasis. *J Immunother Cancer*. 2021;9(1):e001481.

Investigative Ophthalmology & Visual Science